ELSEVIER

Journal of Hazardous Materials B69 (1999) 217–227

Journal of Hazardous Materials

www.elsevier.nl/locate/jhazmat

An approach for evaluating aerosol particle deposition from a natural convection flow onto a vertical flat plate

R. Tsai *, Z.Y. Lin

Department of Mechanical Engineering, Chung Yuan Christian University, Chung Li 320, Taiwan, ROC

Received 24 September 1998; received in revised form 20 May 1999; accepted 2 June 1999

Abstract

An approach through numerical integration for evaluating aerosol particle deposition onto a vertical flat plate is proposed. The airflow was based on the assumption of a two-dimensional, incompressible and steady state laminar flow driven by a buoyancy force. The mechanisms of particle deposition were coupled from natural convection, Brownian diffusion, thermophoresis and electrophoresis due to constant electric strength. This approach demonstrated an easier method of prediction and produced a very good agreement with the thermophoresis exact solution. Results described the role of thermophoretic and electrophoretic forces on particle deposition. The thermophoresis effect was predicted to be particularly important for particles of $d_p \geq 0.1$ μm moving toward a cold surface or away from a hot surface at a given temperature gradient. The electrophoresis effect dominates the deposition of submicron particles.

Keywords: Particle deposition; Natural convection; Brownian diffusion; Thermophoresis; Electrophoresis

1. Introduction

Studies in aerosol particle deposition onto a wall surface due to thermophoresis and/or electrophoresis have gained importance for engineering applications. Particle deposition onto indoor surfaces is one of the technological problems, especially in a typical clean room operation. Commonly, the particle deposition mechanisms considered

* Corresponding author. Tel.: +886-3-4563171-4304; fax: +886-3-4563160; e-mail: rueyyih@cycu.edu.tw

0304-3894/99/$ - see front matter
PII: S0304-3894(99)00108-9

include diffusion, convection, thermophoresis, sedimentation and electrophoresis. In engineering practice, usually more than one mechanism can act simultaneously and their interactions must be considered for the accurate prediction of deposition rates. In this work, the mechanism of particle deposition onto a vertical surface by the coupled effects of diffusion, thermophoresis and electrophoresis was examined. These mechanisms are important for submicron particles.

The significant role of thermophoresis in enhancing small particles moving toward cold surfaces and away from hot surfaces is especially effective for particles with a size of $0.1\ \mu m \leq d_p \leq 10\ \mu m$. Goren [1] developed the thermophoretic deposition of particles in a laminar compressible boundary layer flow past a flat plate. There have been some other works on particle deposition onto a flat plate involving the transport mechanisms of Brownian diffusion and thermophoresis [2–4]. Batchelor and Shen [5,6] used a similarity method to analyze the deposition rates from the effect of thermophoresis in the flow over a flat plate, cylinder and body of revolution.

Work on the mechanisms of Brownian diffusion or inertia and electrophoresis has been presented. Peters et al. [7], Turner et al. [8], and Cooper et al. [9] stated the importance of electrostatic forces on particles onto surfaces in an axisymmetrical viscous stagnation-point flow. Electrostatic forces primarily arise from the coulombic force between a charged particle and a charged collecting surface and the image force between a charged particle and an electrically conducting surface.

For studies on the combined effects of thermophoresis and electrophoresis, Peterson et al. [10] used the boundary layer approximation and perturbation methods to solve the transport equation and determine particle deposition. Peters and Cooper [11] analyzed the effects of electrostatic forces on thermophoretic suppression of particle diffusion deposition onto hot surfaces. Opiolka et al. [12] carried out experiments and used a simple stagnant film model to examine the deposition rates. Tsai et al. [13] developed a theoretical model to predict particle deposition onto a wafer using the coupling effects of thermophoresis and electrophoresis.

There have been relatively few published papers on the rate of thermophoretic particle deposition onto a solid surface in a flow system with natural convection. Mills and Wassel [14] and Nazaroff et al. [15] used a similarity transformation to obtain the deposition rates due to the coupling of thermophoresis and natural convection. In this study, we developed an approach to describe particle transport due to the coupling effects of thermophoresis and electrophoresis from a natural convection flow over a vertical flat plate. This method was based on the similarity analysis associated with a numerical integration scheme for the nonsimilar particle equation.

2. Similarity analysis

2.1. Flow and temperature fields

For this two-dimensional natural convection system, the coordinates were x measured along the surface and y perpendicular to the system. The corresponding velocity components were u and v, respectively. The vertical plate surface was maintained at a

temperature, T_w, and the ambient air was at a different temperature, T_e, in which $T_e > T_w$ for a cold surface and $T_e < T_w$ for a hot surface. For the steady laminar flow, the governing conservation equations of mass, momentum and energy in for natural convection with the Boussinesq approximation are

$$\text{Mass:}\quad \frac{\partial u}{\partial x} + \frac{\partial v}{\partial y} = 0 \tag{1}$$

$$\text{Momentum:}\quad u\frac{\partial u}{\partial x} + v\frac{\partial u}{\partial y} = v_g\frac{\partial^2 u}{\partial y^2} + g\beta(T - T_e) \tag{2}$$

$$\text{Energy:}\quad u\frac{\partial T}{\partial x} + v\frac{\partial T}{\partial y} = \alpha\frac{\partial^2 T}{\partial y^2} \tag{3}$$

where β is the coefficient of thermal volumetric expansion of fluid ($\beta = 1/T$ and here $T = T_e$ for an ideal gas). The boundary conditions at $y = 0$ and $y \to \infty$ are

$$y = 0,\ u = v = 0,\ T = T_w;\ \ y \to \infty,\ u = 0,\ T = T_e \tag{4}$$

The governing equations may be described by a dimensionless stream function $f(\eta)$ and dimensionless temperature $\theta(\eta)$ defined as

$$f(\eta) = \frac{\psi}{cv_g x^{3/4}};\ \theta(\eta) = \frac{T - T_e}{T_w - T_e} = \frac{T - T_e}{\Delta T} \tag{5}$$

where $\eta = cyx^{-1/4}$ and $c = (g\beta|\Delta T|/v_g^2)^{1/4}$. The governing equations with boundary conditions after the similarity transformation for f and θ are

$$f''' + \frac{3}{4}ff'' - \frac{1}{2}f'^2 + \theta = 0 \tag{6}$$

$$\frac{1}{Pr}\theta'' + \frac{3}{4}f\theta' = 0 \tag{7}$$

and

$$f(0) = f'(0) = 0,\ f'(\infty) = 0;\ \ \theta(0) = 1,\ \theta(\infty) = 0 \tag{8}$$

where Pr is the Prandtl number. Solutions for $f(\eta)$ and $g(\eta)$ from the above equations for air ($Pr = 0.72$ used) can be obtained using the methods of quasi-linearization and finite differences.

2.2. Particle concentration field

After the velocity and temperature fields are solved, the particle concentration profiles can be solved from the particle transport equation, including the effects of diffusion, thermophoresis and electrophoresis. We assumed that the particle concentra-

tion was dilute and the particle concentration at the wall zero. Thus, the transport equation associated with the boundary layer assumptions can be expressed as

$$u\frac{\partial N}{\partial x}+\upsilon\frac{\partial N}{\partial y}=D\frac{\partial^2 N}{\partial y^2}-\frac{\partial}{\partial y}\left[(V_{\mathrm{T}}+V_{\mathrm{E}})N\right] \tag{9}$$

with the boundary conditions

$$y=0,\ N=N_{\mathrm{w}}=0;\ \ y\to\infty,\ N=N_{\mathrm{e}} \tag{10}$$

where the velocity V_{E} can be obtained by equating the Stokes drag to the Coulomb force,

$$V_{\mathrm{E}}=-\frac{qCE}{3\pi d_{\mathrm{p}}\mu_{\mathrm{g}}}=-\mu E \tag{11}$$

here q is the charge on the particle, μ_{g} the air viscosity, C the Cunningham correction factor, μ the particle mobility, E the electric field strength. The thermophoretic velocity given by Talbot et al. [16] is

$$V_{\mathrm{T}}=-\kappa\upsilon_{\mathrm{g}}\frac{\nabla T}{T}=-\kappa\upsilon_{\mathrm{g}}\frac{1}{T}\frac{\partial T}{\partial y} \tag{12}$$

The value of $\kappa\upsilon_{\mathrm{g}}$ represents the thermophoretic diffusivity, where κ is the thermophoretic coefficient that is a function of the particle size and materials (see Batchelor and Shen [5] for a suggestion) and υ_{g} is the air kinematic viscosity. A representative value for particles smaller than 1 μm is 0.5. We introduced a thermophoretic parameter $\tau=-\kappa(T_{\mathrm{w}}-T_{\mathrm{e}})/T$, with $\tau=0.01$, 0.05 and 0.1, in which the corresponding values for $-\kappa(T_{\mathrm{w}}-T_{\mathrm{e}})$ were approximately 3, 15, and 30 K for a reference temperature $T=293$ K.

The transformation of Eq. (9) with constant electric field strength in terms of the dimensionless concentration $\phi=N/N_{\mathrm{e}}$ becomes a nonsimilar form

$$\frac{1}{Sc}\phi''+\left[\frac{3}{4}f-\left(\frac{x^{1/4}}{\upsilon_g c}V_{\mathrm{E}}\right)\right]\phi'-\tau(\phi\theta')'-\frac{1}{T}\phi\theta'^2=xf'\frac{\partial\phi}{\partial x} \tag{13}$$

with the boundary conditions

$$\eta=0,\ \phi=0;\ \eta\to\infty,\ \phi=1 \tag{14}$$

where the primes denote partial differentiation with respect to η.

By introducing a dimensionless distance $\xi=x/L$ and dimensionless velocity υ_{g}/L with a reference length L, Eq. (13) becomes

$$\frac{1}{Sc}\phi''+\left[\frac{3}{4}f-\left(\frac{\xi}{Gr_{\mathrm{L}}}\right)^{1/4}\frac{V_{\mathrm{E}}}{\upsilon_{\mathrm{g}}/L}\right]\phi'-\tau(\phi\theta')'-\frac{1}{T}\phi\theta'^2=\xi f'\frac{\partial\phi}{\partial\xi} \tag{15}$$

Although the above equation is still a partial differential equation, the solution obtained for it in the numerical work is easier than Eq. (9), as mentioned in the book by Cebeci and Bradshaw [17].

3. Particle deposition velocity

In the mass transfer analysis, the particle flux is determined using the definition

$$J = -D\frac{\partial N}{\partial y} + (v + V_T + V_E)N$$

and the deposition flux at the wall surface is

$$J_s = -D\frac{\partial N}{\partial y}\bigg|_{y=0} = -D\phi'(0)N_e c x^{-1/4} \tag{16}$$

The deposition velocity is customarily defined as the particle flux divided by the free stream concentration,

$$V_d = \frac{J_s}{N_e} = -D\phi'(0)\left[\frac{Gr_L}{\xi}\right]^{1/4}\frac{1}{L} \tag{17}$$

or with a reference velocity v_g/L, a dimensionless velocity is defined as

$$V_d^* = \frac{V_d}{v_g/L} = -\frac{1}{Sc}\phi'(0)\left[\frac{Gr_L}{\xi}\right]^{1/4} \tag{18}$$

Usually, the particle Schmidt number for aerosols is very large ($\geq 10^3$) and the resulting concentration boundary layer is much thinner than the hydrodynamic and thermal boundary layers. Because of $\partial N/\partial x \ll \partial N/\partial y$ in the concentration boundary layer, using the analysis of the orders of magnitude, the effect due to the terms on the right-hand side of Eq. (15) is insignificant (this leads the maximum possible error checked to be about 2% for submicron particles). The last term on the left-hand side of Eq. (15) is a higher-order term and can be negligible at normal temperatures. Thus, an asymptotic solution may be found in the concentration layer in which the velocity and temperature profiles are assumed to be linear. Therefore, f and θ' in Eq. (15) with negligible higher terms can be approximated using the first term of expansion, $f = f''(0)\eta^2/2$ and $\theta' = \theta'(0)$, yielding

$$\frac{1}{Sc}\phi'' + \left(\frac{3}{8}f''(0)\eta^2 - \tau\theta'(0) - \left[\frac{\xi}{Gr_L}\right]^{1/4}\frac{V_E}{v_g/L}\right)\phi' = 0 \tag{19}$$

Integrating this equation produces concentration profiles $\phi(\eta)$ and the gradient at the wall $\phi'(0)$ as

$$\phi(\eta) = \frac{\displaystyle\int_0^{\eta}\exp\left[Sc\left(-\frac{1}{8}f''(0)\zeta^3 + \tau\theta'(0)\zeta + \left[\frac{\xi}{Gr_L}\right]^{1/4}\frac{V_E}{v_g/L}\zeta\right)\right]d\zeta}{\displaystyle\int_0^{\infty}\exp\left[Sc\left(-\frac{1}{8}f''(0)\zeta^3 + \tau\theta'(0)\zeta + \left[\frac{\xi}{Gr_L}\right]^{1/4}\frac{V_E}{v_g/L}\zeta\right)\right]d\zeta} \tag{20}$$

and

$$\phi'(0) = \frac{1}{\int_0^\infty \exp\left[Sc\left(-\frac{1}{8}f''(0)\zeta^3 + \tau\theta'(0)\zeta + \left[\frac{\xi}{Gr_L}\right]^{1/4}\frac{V_E}{\upsilon_g/L}\zeta\right)\right]\mathrm{d}\zeta} \tag{21}$$

Eq. (18) together with Eq. (21) are quite useful in determining the deposition rates for a given particle size because the unknown quantity is only $\phi'(0)$; thus, there is no need to determine the concentration gradient by numerically integrating the concentration profile. $f''(0) = 0.96324$ and $\theta'(0) = -0.36162$ obtained are from solving Eqs. (6)–(8)).

4. Results and discussion

The dimensionless particle deposition velocity in Eq. (18), V_d^*, is only a function of the slope of the concentration profile at the wall $\phi'(0)$ and the particle Schmidt number as Gr_L and ξ are known, while the concentration profiles depend on the thermophoretic parameter. There have been two ways to determine the value of $\phi'(0)$. One is a direct method from a similar particle concentration profile solution and the other is from the approach in Eq. (21).

Particles were selected in a range of 0.01–10 μm corresponding to the value of the Schmidt number from 2.87×10^2 to 6.20×10^6 [18]. To demonstrate the accuracy for the approach using Eq. (21), Table 1 is a comparison of prediction deposition velocities for $x = 1$ m, $T_e = 293$ K and $\kappa = 0.5$ between the approach of Eq. (21) and similarity solutions (presented by Nazaroff and Cass [15]). The table shows that the agreement is very good in which the maximum possible error is less than 2%. The similarity solutions may be called exact. However, the concentration profiles in the boundary layer must be solved first, which requires the use of a numerical scheme in solving the differential equations. The approach of Eq. (21) is an easier way in determining particle deposition velocities by using only a simple numerical integration. Thus, we adopted that approach to examine the deposition rates due to the coupling of diffusion, thermophoresis and electrophoresis.

Table 1
A comparison of $V_d \times 10^4$ cm s^{-1} given by Exact[a] and Approach[b]

		$T_w - T_e$ (K)									
d_p (μm)		−10	−4	−2	−1	−0.1	0.1	1	2	4	10
0.01	Exact	47.3	32.6	25.7	21.0	11.5	11.5	19.9	23.0	25.8	26.9
	Approach	48.5	33.2	26.4	21.6	11.8	11.8	20.5	23.7	26.6	28.0
0.1	Exact	18.0	6.1	3.0	1.8	0.68	0.62	0.66	0.39	0.07	–
	Approach	18.3	6.16	3.07	1.81	0.68	0.62	0.66	0.39	0.07	–
1.0	Exact	17.9	5.7	2.4	1.0	0.11	0.05	–	–	–	–
	Approach	18.0	5.77	2.43	1.03	0.11	0.05	–	–	–	–

[a] Data are taken from Nazaroff's paper [15].
[b] Present results.

4.1. Effect of electrophoresis

Electrophoresis on the particles can play an important role in the rate of particle deposition onto a surface in a clean environment. The resulting Coulombic forces, like the diffusive and thermophoretic forces, can influence the particle concentration profiles and deposition rates. There are numerous mechanisms for establishing an electric field around a surface and for imparting charges to the particles. For simplicity, we only considered particles with uniform charges and under the influence of a uniform electric field; that is, the electrophoretic velocity is assumed to be constant. Therefore, the Coulombic forces can be described by the product φE, which accounts for the particle charge and the electric field strength. A surface that induces an electric strength of 1 kVcm^{-1} will result in the product φE of the order of ± 0–10^5 Vcm^{-1}. Thus, Coulombic attraction can enhance the deposition of submicron particles by several orders of magnitude.

To examine the effect of electrophoretic force due to electric field strength, the characteristic values for φE selected were 10, 10^2, and 10^3 Vcm^{-1}, under a clean room environment [8]. For a cold surface, Fig. 1 shows the calculated deposition velocities for particles of 0.01–10 μm at $\xi = 1.0$ and different ΔT under the influence of $\varphi E = 10^2$ Vcm^{-1}. Fig. 2 shows a comparison of deposition velocities at $\Delta T = -1$ K and three different φE. For small particles ($d_p \leq 0.1$ μm), the deposition velocities are primarily due to the effects of Brownian diffusion and electrophoresis; yet, the effect of thermophoresis plays an important role for larger particles. It can be seen that the deposition

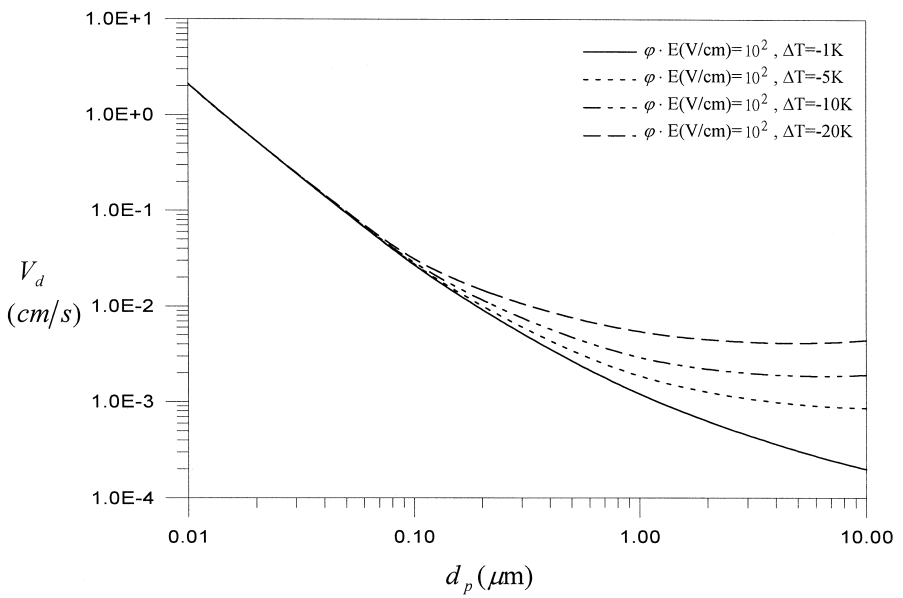

Fig. 1. Particle deposition velocities for $\varphi E = 10^2$ V cm^{-1} and $\Delta T < 0$ at $\xi = 1.0$ and $L = 1.0$ m.

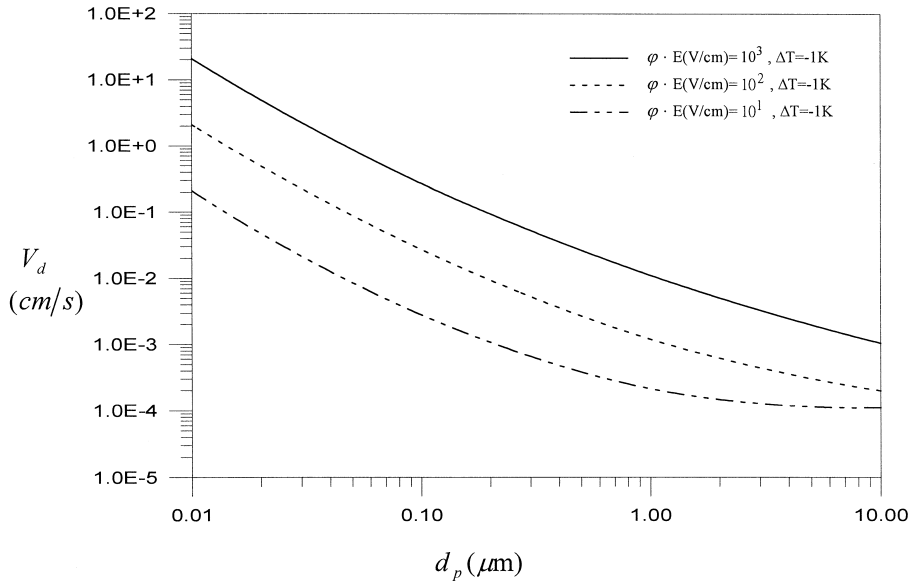

Fig. 2. Particle deposition velocities for $\Delta T = -1$ K and three different φE at $\xi = 1.0$ and $L = 1.0$ m.

velocities decrease with increasing particle size, primarily by reducing the effect of Brownian diffusion.

For a hot surface, Figs. 3 and 4 show the calculated particle deposition velocities at $\xi = 1.0$ and different ΔT under the influence of $\varphi E = 10^2$ and 10^3 Vcm^{-1}, respectively. For $d_p \geq 0.1$ μm, the effect from Brownian diffusion may be negligible because it is relatively small compared to the thermophoretic and electrophoretic effects. However, the forces by thermophoresis and electrophoresis act upon the particles in opposite directions. Thus, if $V_T + V_E < 0$, a dust-free zone occurs (not shown) and V_d approached zero (as shown in Figs. 3 and 4).

When we examined the influence of electrophoresis onto particle deposition velocity in the case of particles of a fixed diameter, Eq. (11) implies that the electrophoretic velocity is proportional to the applied electric field strength and inversely proportional to the particle diameter. From Figs. 1 and 3, it is seen that the predicated curves are approximately proportional to d_p^{-1}, which indicates that electrophoresis is the dominating mechanism. However, the curves deviate from d_p^{-1} law at particles of $d_p \cong 0.1$ μm because of the influence of thermophoresis. Figs. 2 and 5 are plots of calculated deposition velocities for $|\Delta T| = 1$ K and three different values of φE. For particles of $d_p =$ 0.01 μm, since the electrophoretic force is the dominating mechanism which moves particles toward the surface, it can be seen that the predicated deposition velocities are approximately proportional to the applied φE. However, when particle size is increased, the influence of the convection flow and thermophoresis upon particle deposition is more complicated. For particles of $d_p = 1.0$ μm with smaller elec-

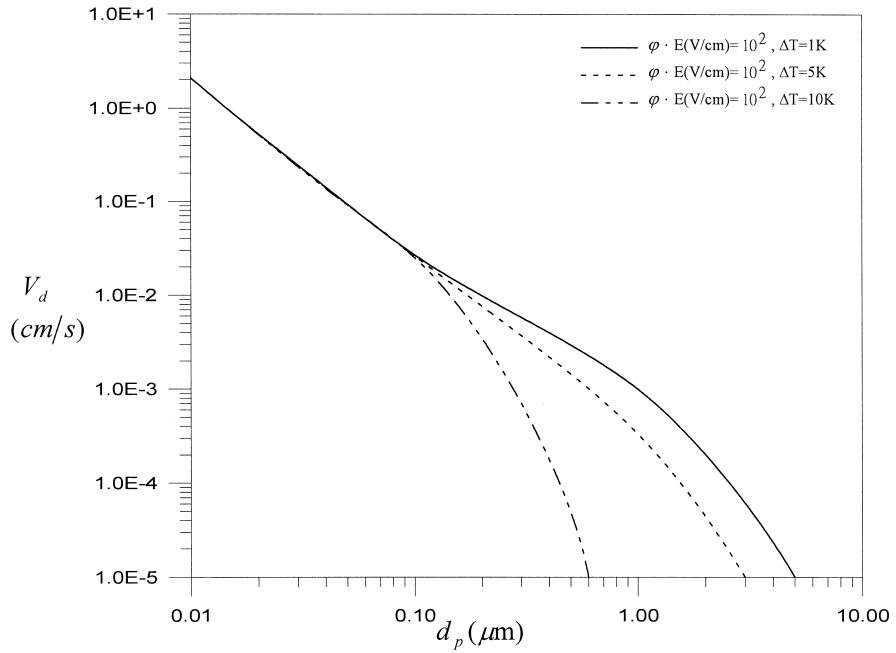

Fig. 3. Particle deposition velocities for $\varphi E = 10^2$ V cm^{-1} and $\Delta T > 0$ at $\xi = 1.0$ and $L = 1.0$ m.

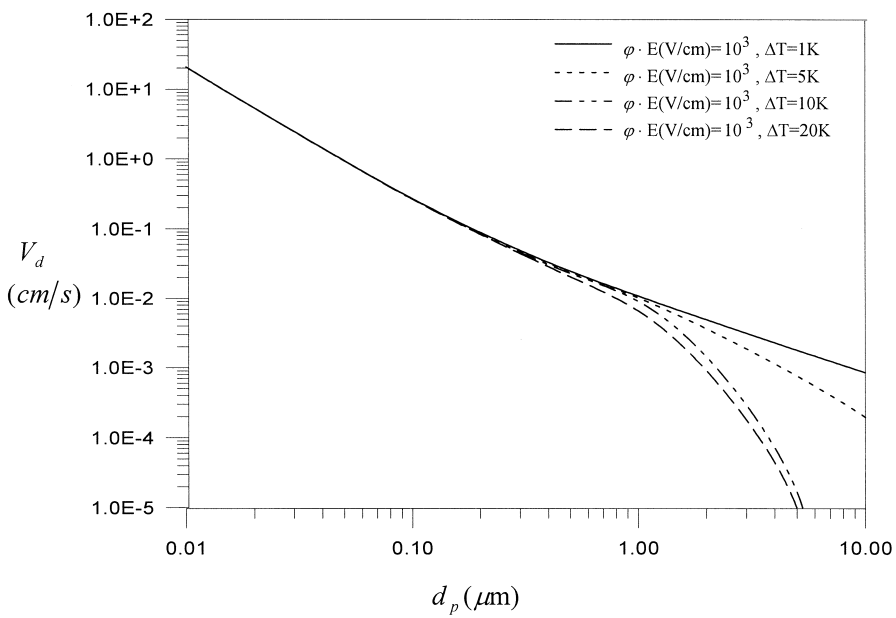

Fig. 4. Particle deposition velocities for $\varphi E = 10^3$ V cm^{-1} and $\Delta T > 0$ at $\xi = 1.0$ and $L = 1.0$ m.

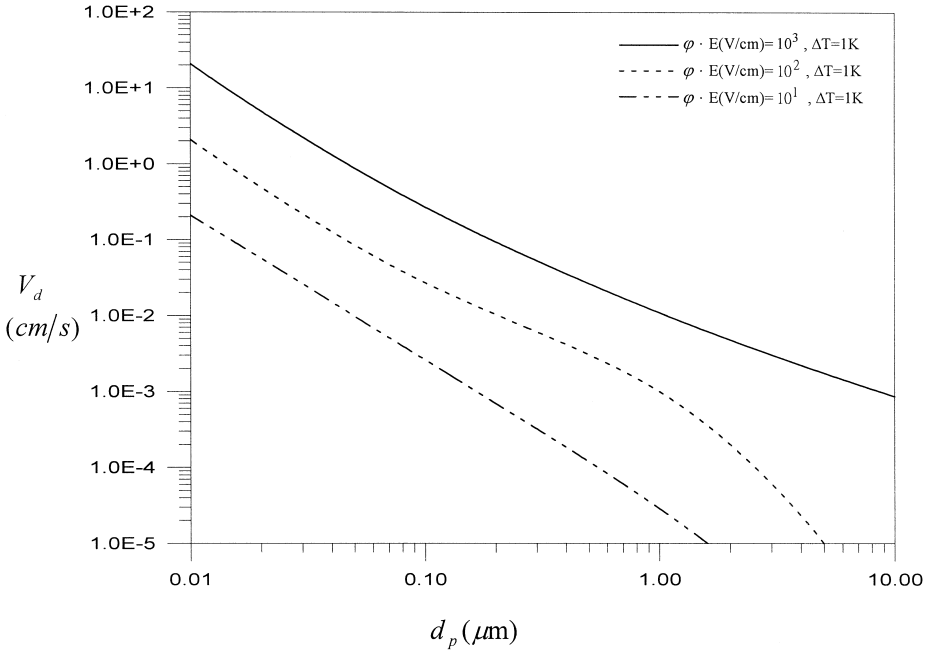

Fig. 5. Particle deposition velocities for $\Delta T = 1$ K and three different φE at $\xi = 1.0$ and $L = 1.0$ m.

trophoretic forces applied ($\varphi E = 10^2$ and 10^1 Vcm^{-1}), the deposition velocities for hot surfaces are less than for cold surfaces even though ΔT is only 1 K.

5. Conclusions

An approach was developed to describe particle transport in a thermally driven natural convection for a vertical flat plate. The particle flux to the surface is expressed in terms of the particle deposition velocity. The model includes transport due to natural convection, diffusion, thermophoresis and electrophoresis. An integral solution for the deposition velocity, with the assumptions of linear velocity and temperature profiles in the concentration boundary layer and constant electric strength, is available. This approach demonstrated an easier method of prediction and a very good agreement with the exact solutions for the thermophoresis effect.

Results were presented to describe the role of thermophoretic and electrophoretic forces on particle deposition. Even when the temperature difference between the wall and the ambient air is only 1 K, thermophoresis plays an important role for particles of $d_p \geq 0.1$ μm and the influence of thermophoresis increases with an increase in the difference. Coulombic forces dominate the deposition of submicron particles even when the surface carries only a relatively weak electric potential.

Acknowledgements

The authors are grateful to the National Science Council, Taiwan, ROC for support through grant No. NSC-88-2211-E-033-002.

References

[1] S.L. Goren, J. Colloid Interface Sci. 61 (1977) 77.
[2] G.M. Homsy, F.T. Geyling, K.L. Walker, J. Colloid Interface Sci. 83 (1981) 495.
[3] J.M. Hales, L.C. Schwendiman, T.W. Horst, Int. J. Heat Mass Transfer 15 (1972) 1837.
[4] A.F. Mills, X. Hang, F. Ayazi, Int. J. Heat Mass Transfer 25 (1984) 665.
[5] G.K. Batchelor, C. Shen, J. Colloid Interface Sci. 107 (1985) 21.
[6] C. Shen, J. Colloid Interface Sci. 127 (1989) 104.
[7] M.H. Peters, D.W. Cooper, R.J. Miller, J. Aerosol Sci. 20 (1989) 123.
[8] J.R. Turner, D.K. Liguras, H. Fissan, J. Aerosol Sci. 20 (1989) 403.
[9] D.W. Cooper, M.H. Peters, R.J. Miller, Aerosol Sci. Technol. 11 (1989) 133.
[10] T.W. Peterson, F. Stratmann, H. Fissan, J. Aerosol Sci. 20 (1989) 683.
[11] M.H. Peters, D.W. Cooper, J. Colloid Interface Sci. 140 (1990) 48.
[12] S. Opiolka, F. Schmidt, H. Fissan, J. Aerosol Sci. 25 (1994) 665.
[13] R. Tsai, Y.P. Chang, T.Y. Lin, J. Aerosol Sci. 29 (1998) 811.
[14] A.F. Mills, A.T. Wassel, Letters in Heat Mass Transfer 2 (1975) 159.
[15] W.W. Nazaroff, G.R. Cass, J. Aerosol Sci. 18 (1987) 445.
[16] L. Talbot, R.K. Cheng, R.W. Scheffer, D.P. Wills, J. Fluid. Mech. 101 (1980) 737.
[17] T. Cebeci, P. Bradshaw, Physical and Computational Aspects of Convective Heat Transfer, Springer-Verlag, New York, 1984, p. 76.
[18] S.K. Friedlander, Smoke, Dust and Haze, Wiley, New York, 1977, p. 32.